AD-A038 899 NAVAL POSTGRADUATE SCHOOL MONTEREY CALIF F/G 4/2
AN INVESTIGATION OF SMALL SCALE HUMIDITY FLUCTUATIONS IN THE MA--ETC(U)
DEC 76 W L SHUTT

UNCLASSIFIED NL

1 OF 1
AD
A038899

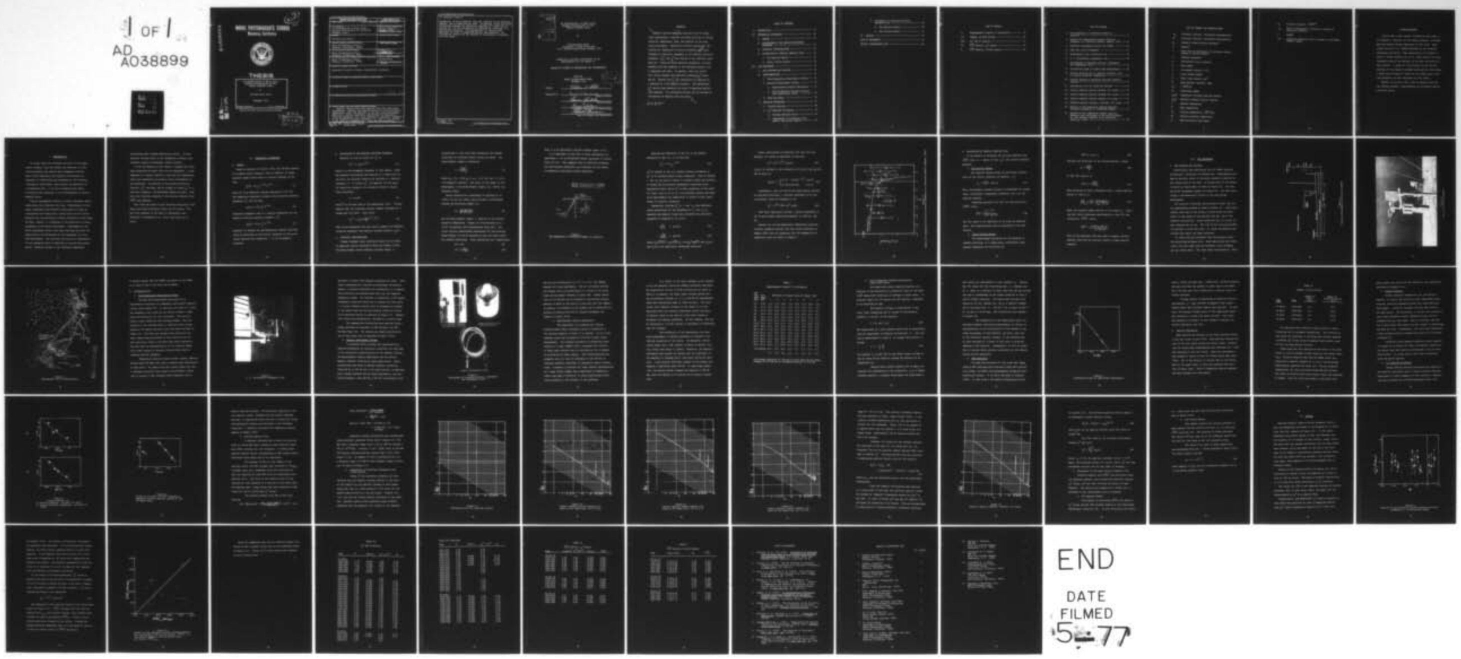

END
DATE
FILMED
5-77

NAVAL POSTGRADUATE SCHOOL
Monterey, California

THESIS

AN INVESTIGATION OF SMALL SCALE HUMIDITY FLUCTUATIONS IN THE MARINE BOUNDARY LAYER

by

William Leroy Shutt

December 1976

Thesis Advisor: K. L. Davidson

SECURITY CLASSIFICATION OF THIS PAGE (When Data Entered)

REPORT DOCUMENTATION PAGE		READ INSTRUCTIONS BEFORE COMPLETING FORM
1. REPORT NUMBER	2. GOVT ACCESSION NO.	3. RECIPIENT'S CATALOG NUMBER
4. TITLE (and Subtitle) An Investigation of Small Scale Humidity Fluctuations in the Marine Boundary Layer		5. TYPE OF REPORT & PERIOD COVERED Master's Thesis; December 1976
		6. PERFORMING ORG. REPORT NUMBER
7. AUTHOR(s) William Leroy Shutt		8. CONTRACT OR GRANT NUMBER(s)
9. PERFORMING ORGANIZATION NAME AND ADDRESS Naval Postgraduate School Monterey, California 93940		10. PROGRAM ELEMENT, PROJECT, TASK AREA & WORK UNIT NUMBERS
11. CONTROLLING OFFICE NAME AND ADDRESS Naval Postgraduate School Monterey, California 93940		12. REPORT DATE December 1976
		13. NUMBER OF PAGES 63
14. MONITORING AGENCY NAME & ADDRESS(if different from Controlling Office) Naval Postgraduate School Monterey, California 93940		15. SECURITY CLASS. (of this report) Unclassified
		15a. DECLASSIFICATION/DOWNGRADING SCHEDULE

16. DISTRIBUTION STATEMENT (of this Report)

Approved for public release; distribution unlimited.

17. DISTRIBUTION STATEMENT (of the abstract entered in Block 20, if different from Report)

18. SUPPLEMENTARY NOTES

(C sub T) squa

251 450

19. KEY WORDS (Continue on reverse side if necessary and identify by block number)

20. ABSTRACT (Continue on reverse side if necessary and identify by block number)

Humidity spectra have been measured with the Lyman-alpha humidiometer, together with mean profiles of virtual potential temperature, wind, and humidity in the open ocean environment. Empirically derived expressions describing the temperature structure parameter, C_T^2, were extended by similarity arguments to the humidity-structure parameter, C_q^2, and C_q^2 was related to the stability parameter Ri. Using the above measured

(cont on p. 2)

DD FORM 1 JAN 73 1473 EDITION OF 1 NOV 65 IS OBSOLETE
(Page 1) S/N 0102-014-6601 |

SECURITY CLASSIFICATION OF THIS PAGE (When Data Entered)

20. Abstract (Cont'd)

parameters, vertical humidity flux was computed in two different manners, and a comparison was made. In general, there was little correlation between the spectrally analyzed C_q^2 values and Ri. Results for C_q^2 can essentially be regarded as a function of z and humidity gradient. Non-dimensional C_q^2 results were generally an order of magnitude smaller than expected. No correlation between the two methods of calculation of humidity flux was found.

An Investigation of Small Scale Humidity Fluctuations in the Marine Boundary Layer

by

William Leroy Shutt
Lieutenant, United States Navy
B.S., United States Naval Academy, 1971

Submitted in partial fulfillment of the requirements for the degree of

MASTER OF SCIENCE IN METEOROLOGY AND OCEANOGRAPHY

from the

NAVAL POSTGRADUATE SCHOOL
December 1976

Author: William L. Shutt

Approved by: Kenneth L. Davidson, Thesis Advisor

Thomas Houlihan, Second Reader

George J. Haltiner, Chairman, Department of Meteorology

Robert R. Fossum, Dean of Science and Engineering

ABSTRACT

Humidity spectra were ~~have been~~ measured with the Lyman-alpha humidiometer, together with mean profiles of virtual potential temperature, wind, and humidity in the open ocean environment. Empirically derived expressions describing the temperature structure parameter~~, C_T^2,~~ were extended by similarity arguments to the humidity-structure parameter, C_q^2, and C_q^2 was related to the stability parameter Ri. Using the above measured parameters, vertical humidity flux was computed in two different manners, and a comparison was made. In general, there was little correlation between the spectrally analyzed C_q^2 values and Ri. Results for C_q^2 can essentially be regarded as a function of z and humidity gradient. Non-dimensional C_q^2 results were generally an order of magnitude smaller than expected. No correlation between the two methods of calculation of humidity flux was found.

(C sub q) Squared

TABLE OF CONTENTS

LIST OF TABLES

LIST OF FIGURES

LIST OF SYMBOLS AND ABBREVIATIONS

α_q	Universal constant, determined experimentally
β	Universal constant, determined experimentally
C_q	Humidity index-structure parameter
ρ	Density
ϵ	Mean rate of dissipation of turbulent kinetic energy by viscous effects
f	Temporal frequency
g	Acceleration due to gravity
k	Wave number
κ	von Karman constant, 0.35
ℓ	Local mixing length
Q	Water vapor density, gm^{-3}
$\overline{q}$	Mean specific humidity, g/kg
q_*	$= \overline{-w'q'}/U_*$
Ri	Richardson number
$S_T(k)$	Temperature variance spectral density
$S_q(k)$	Humidity variance spectral density
T	Ambient temperature
$\overline{T}$	Mean temperature
T_*	Scaling temperature, $(\overline{-w'T'}/U_*)$
Θv	Virtual potential temperature
$\overline{U}$	Mean horizontal wind speed

U_*	Friction velocity, $(\overline{-u'w'})^{\frac{1}{2}}$
χ_q	Rate of dissipation of humidity variance by molecular diffusion
z	Height
z/L	Stability parameter ratio of height to the Monin-Obukhov length

ACKNOWLEDGEMENTS

I would like to give special recognition and thanks to Dr. Kenneth L. Davidson for his expert guidance, encouragement and support during completion of this study. Many thanks also go to Dr. Thomas Houlihan for his technical assistance and advice. Much appreciation is extended to both Dr. Gordon Schacter and to Dr. Chris Fairall for their invaluable help in the analysis of the data collected for this project. I thank Mr. Steve Rinard for his careful analysis of the computer programs developed for this thesis. I thank also LT George W. Karch for providing some of the data necessary for the completion of this thesis.

Finally, to my wife, Judy, goes my deepest gratitude. Her endless patience, understanding and assistance made my work much easier.

I. INTRODUCTION

In recent years the turbulent structure of the atmospheric boundary layer has become very important to both electro-magnetic and optical wave propagation studies. Small scale temperature and humidity fluctuations are important in determining such phenomena as the intensity, fluctuation, beam wander, beam spread, and absorption of a transmitted wave. It is also recognized that these fluctuations are important in the understanding of electro-magnetic waves.

Initial experimental efforts to verify turbulence theory predictions were conducted over land. Measurements of wind speed, temperature and humidity fluctuations in those investigations were taken from a stable platform with instrumentation not encountering as severe conditions as were these. The Navy, however, is interested in the prediction of these parameters in the marine environment. Experiments at the Naval Postgraduate School have been providing the basis for predictions of the properties of the atmosphere for relevant wavelengths. The turbulent fluctuation of temperature is that parameter which is important in optical wave propagation. Numerous studies of the turbulent temperature

fluctuations have yielded significant results. In this analysis, another facet of the atmospheric boundary layer turbulent regime is considered, namely humidity.

It was the purpose of this thesis to examine the turbulence properties of water vapor in the atmosphere. It was examined in a fashion similar to that used for temperature, since both parameters are passive scalar contaminants in the atmosphere. An analysis of the humidity-structure function, C_q^2, was made, and an attempt to relate C_q^2 to a stability parameter, the Richardson number was made. Likewise, the turbulent transfer of the vertical humidity flux ($\overline{w'q'}$) was examined.

This study was based on data obtained during April 1976 under open ocean conditions aboard the R/V Acania. The data were examined on the basis of expressions used previously by Wyngaard et al. (1971) and Friehe et al, (1975).

II. THEORETICAL BACKGROUND

A. GENERAL

Based on analyses of Corrsin (1951) the variance spectra of a passive scalar property, such as humidity, at large Reynolds numbers should have an inertial subrange of the form

$$S_q(k) = \beta \chi_q \, \epsilon^{-1/3} \, k^{-5/3} \quad , \qquad (1)$$

where β is an empirical constant evaluated to be 0.25. The temperature spectrum in terms of the structure function parameter $C_T^{\,2}$, has the form

$$S_T(k) = 0.25 \, C_T^{\,2} \, k^{-5/3} \quad . \qquad (2)$$

Similarity arguments lead to a parallel expression for the humidity structure function parameter, $C_q^{\,2}$

$$S_q(k) = 0.25 \, C_q^{\,2} \, k^{-5/3} \quad . \qquad (3)$$

Equation (3) defines the one-dimensional humidity spectrum which by definition is the Fourier transform of the correlation function with separation r in the streamwise direction.

B. CALCULATION OF THE HUMIDITY-STRUCTURE PARAMETER

Equation (3) can be solved for $C_q^{\,2}$ as

$$C_q^{\,2} = 4\, S_q(k)\, k^{5/3} \tag{4}$$

where k is the streamwise component of wave number. Since the humidity fluctuations are measured at a fixed point in the flow, the resultant spectra are realized at a temporal frequency, f. To obtain $C_q^{\,2}$, the temporal (f) and space (k) scales are assumed to be related by Taylor's frozen-field hypothesis,

$$k = 2\pi f/\overline{U} \tag{5}$$

where $\overline{U}$ is the mean wind at the measurement level. "Frozen" implies that the turbulence pattern remains unchanged as it sweeps past the probe. This yields

$$C_q^{\,2} = 4\, S_q(k) \left(\frac{2\pi}{\overline{U}}\right)^{5/3} f^{5/3}. \tag{6}$$

This is the expression that was used to compute the humidity-structure parameter from humidity variance spectra, $S_q(k)$.

C. STABILITY CONSIDERATIONS

Present boundary layer turbulence theory has its basis on empirical results obtained by Monin and Obukhov (1954). The Monin-Obukhov theory defines a scaling length, L,

proportional to the level where mechanical and thermal production of turbulent kinetic energy are equal. The Monin-Obukhov length is defined as

$$L = \frac{T_v {U_*}^2}{q \kappa T_{*v}} \tag{7}$$

where $T_{*v} = T_* + 0.61\, q_* T$, $q_* = -w'q'/U_*$, and $\kappa = 0.35$ (von Karman's constant). The ratio of the height of the measurement to the Monin-Obukhov length, z/L, serves as a stability index.

Recent observational experiments by Businger et al (1971), as well as others, have provided a relationship between the Richardson number, Ri,

$$Ri = \frac{g(\partial \theta v/\partial z)}{\theta(\partial u/\partial z)^2} \tag{8}$$

and the Monin-Obukhov length, L, where θv is the virtual potential temperature. Figure (1) from Businger et al (1971) illustrates this determination quite well. The latter results substantiated expressions for the relationships between z/L and Ri proposed by Dyer and Dicks (1970) for unstable conditions. These expressions are, respectively,

$$z/L = Ri \tag{9}$$

$$z/L = \frac{Ri}{1-\alpha Ri} \tag{10}$$

Here α is an empirically derived constant equal to 0.5.

It is important to note that in these expressions z/L approaches ∞ as the Richardson Number approaches a critical value of 0.21. This suggests that as stability increases, the flow becomes essentially non-turbulent and the effect of mechanical turbulence becomes negligible.

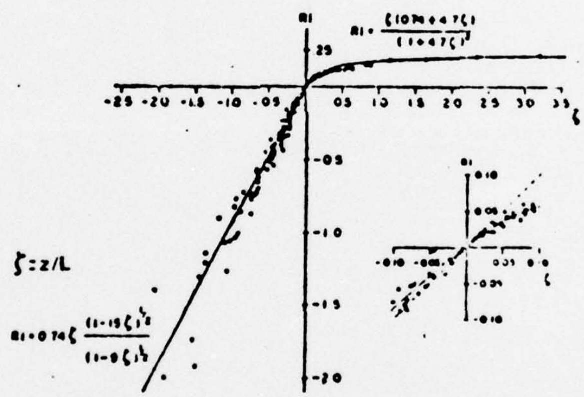

Figure 1.
The dependence of Richardson Number on stability.

Applying the definition of Eqn (4) to the general expression of Eqn (1), it is seen that

$$C_q^{\ 2} = \beta \chi_q \epsilon^{-1/3} \qquad (11)$$

$C_q^{\ 2}$ as defined by Eqn (11) enables indirect estimates of $C_q^{\ 2}$ to be obtained based on mean conditions. This is because ϵ and χ_q are easily related to boundary fluxes and profiles, if steady and horizontally homogeneous conditions exist. Expressions which relate $C_q^{\ 2}$ to mean properties of the boundary layer, such as Ri or z/L, are desirable because the small scale measurements are impractical to obtain in most operational or tactical situations.

Expressions relating $C_q^{\ 2}$ to ϵ and χ_q, and similarity theory predictions for the dependence of ϵ and χ_q on momentum and humidity fluxes were obtained from similarity arguments by Wyngaard et al (1971):

$$\frac{\epsilon}{U_*^{\ 3} z} = f_1(z/L) \qquad (12)$$

$$\frac{\chi_q}{q_* U_* z} = f_2(z/L) \qquad (13)$$

where $U_* = (\overline{-u'w'})^{\frac{1}{2}}$, $q_* = -\overline{w'q'}/U_*$, $L = -T_o U_*^{\ 3}/kg\overline{w'T'}$ and $f_1(z/L)$ and $f_2(z/L)$ are empirically determined functions.

Direct substitution of Equations (12) and (13) into Equation (1) yields an expression of the form

$$C_q^{\ 2} = q_*^{\ 2} \ z^{-2/3} \ f_3(z/L) \ . \qquad (14)$$

$f_3(z/L)$ is defined by the combination of $f_1(z/L)$ and $f_2(z/L)$, and is given by

$$f_3(z/L) = \begin{cases} 4.9 \ [1 - 7(z/L)]^{-2/3} ; & z/L \leq 0 \\ 4.9 \ [1+2.8(z/L)] ; & z/L \geq 0 \end{cases} \qquad (15)$$

Furthermore, since z/L and Ri are functionally related, as described previously, a parallel dependence of Ri can be obtained, which is (Wyngaard et al)

$$C_q^{\ 2} = z^{4/3} (\partial \bar{q} / \partial z)^2 \ f_4(Ri) \qquad (16)$$

This final expression provides a desired dependence of $C_q^{\ 2}$ on more readily measured parameters (z, $\partial \bar{q} / \partial z$), and Ri).

Results for the non-dimensional temperature structure function parameter derived over open ocean conditions by Hughes (1976) and its comparison with the Wyngaard et al prediction curve are shown in Figure 2.

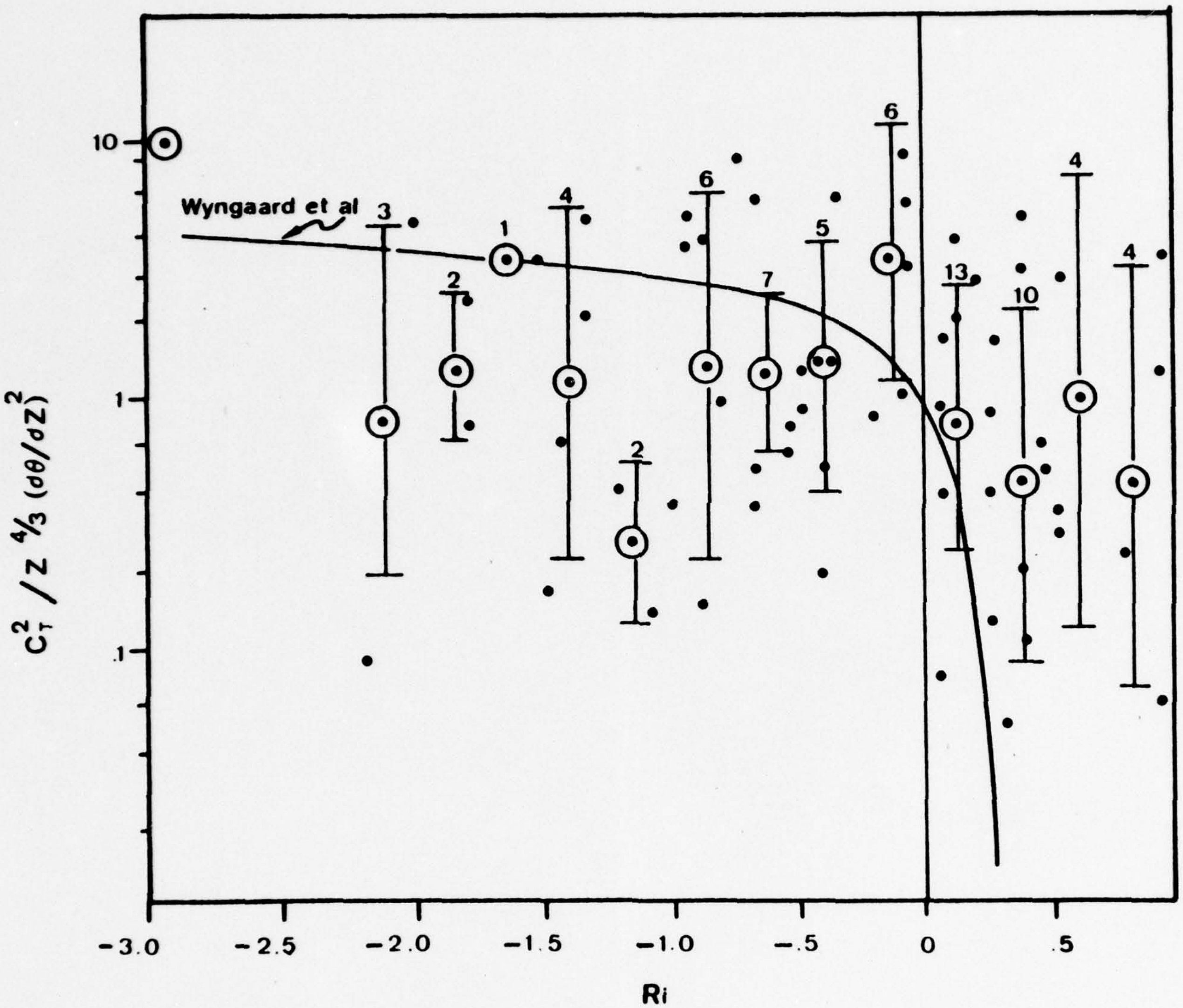

Figure 2.
Results of temperature-structure function parameter vs. Richardson Number (Hughes, 1976)

D. CALCULATION OF VERTICAL HUMIDITY FLUX

It is possible to determine the vertical humidity flux $(\overline{w'q'})$ from measurements of wind, C_q^2, and vertical humidity gradient.

1. The Spectral Method

The spectral method yields the following relationship for the viscous diffusion of humidity, χ_q,

$$\chi_q = (\overline{w'q'})\ \partial \bar{q}/\partial z \tag{17}$$

Here, the humidity variance balance is determined for steady state, horizontally homogeneous conditions, and q is the specific humidity.

Combining Equations (11) and (17) and solving for $(\overline{w'q'})$ yields

$$\overline{w'q'} = \frac{C_q^2\ \epsilon^{1/3}}{0.25\ \partial \bar{q}/\partial z} \tag{18}$$

Eqn (18) needs to be simplified to use with the measured data. This simplification will be described in the next section.

2. Direct Profile Method

The acknowledged expression for the gradient of humidity pertinent to a steady-state, horizontally homogeneous atmosphere can be written as:

$$\partial \overline{q} / \partial z = q_* / \kappa z \tag{19}$$

Applying the definition of the scaling humidity, namely

$$q_* = \frac{-\overline{w'q'}}{U_*} \tag{20}$$

to Eqn (19) results in

$$\partial \overline{q} / \partial z = \frac{-\overline{w'q'}}{\kappa z U_*} \tag{21}$$

When expressed in finite difference form, a simple approximation to $\partial \overline{q} / \partial z$ is

$$\left.\frac{\partial \overline{q}}{\partial z}\right|_{z_3} \approx \frac{\Delta \overline{q}}{\Delta z} = \frac{\overline{q}(z2) - \overline{q}(z_1)}{z_{3\ln} (z_2/z_1)} \tag{22}$$

where the computed number applies to the height z_3. Applying this finite difference approximation to Eqn (21) and solving for $(-\overline{w'q'})$ yields

$$-\overline{w'q'} = \frac{\kappa U_*(\overline{q}(z_2) - \overline{q}(z_1))}{\ln (z_2/z_1)} \tag{23}$$

This is the expression that was used to compute vertical humidity flux from the vertical profile of mean specific humidity.

III. THE EXPERIMENT

A. THE PLATFORM AND LOCATION

Observations were made aboard the R/V ACANIA anchored off Monterey, California in Monterey Bay. Measurements were made at multiple levels on two masts spatially separated on the forward deck of the ship. An illustration of the sensor locations of these masts is shown in Figure (3). The vane and probe arrangement appears in Figure (4). The vane maintained a one-dimensional profile of the wind during measurements.

The location of Monterey Bay provided an ideal site for the experimental program as shown in Figure (5). Open ocean differs from land in the effects of wave action on turbulence, in the nature of the aerosols and fog, and in the humidity fluctuations. These conditions can, of course, be best obtained far at sea. The cost of such activities makes it desirable to work near land. Pt. Pinos and Monterey Bay provide very nearly the ideal situation.

Pt. Pinos projects northwest from the mainland toward the prevailing northwest wind. Even under storm wind conditions, the wind comes from the southwest, still bringing sea air toward shore. The ocean depth surrounding Pt. Pinos

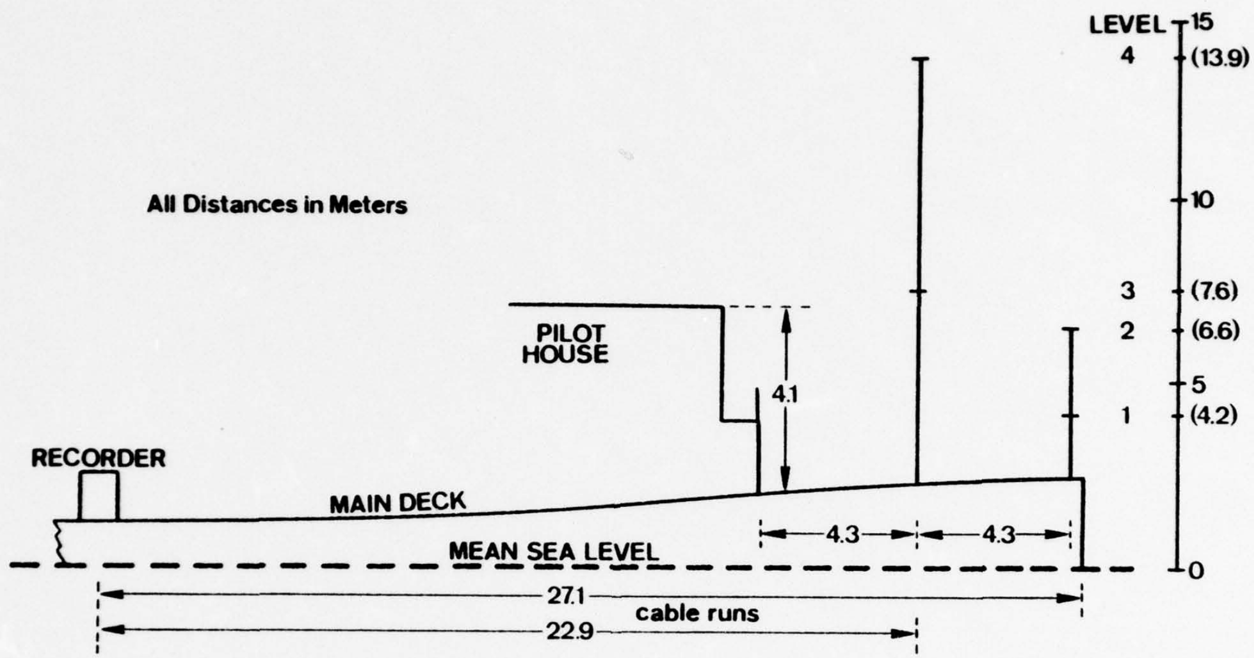

Figure 3.
Mounting arrangements aboard the ACANIA

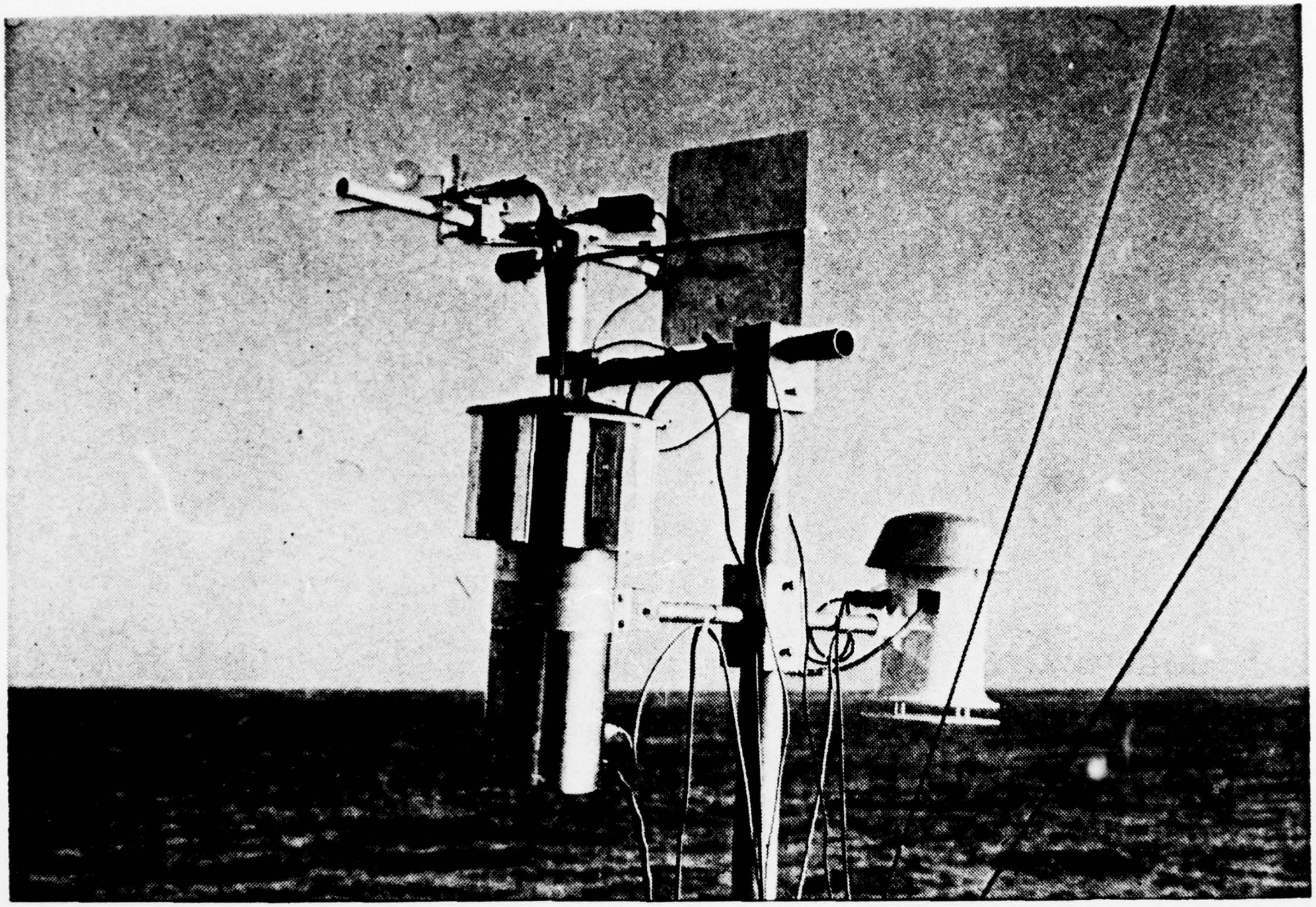

Figure 4.
Vane and Probe Arrangement

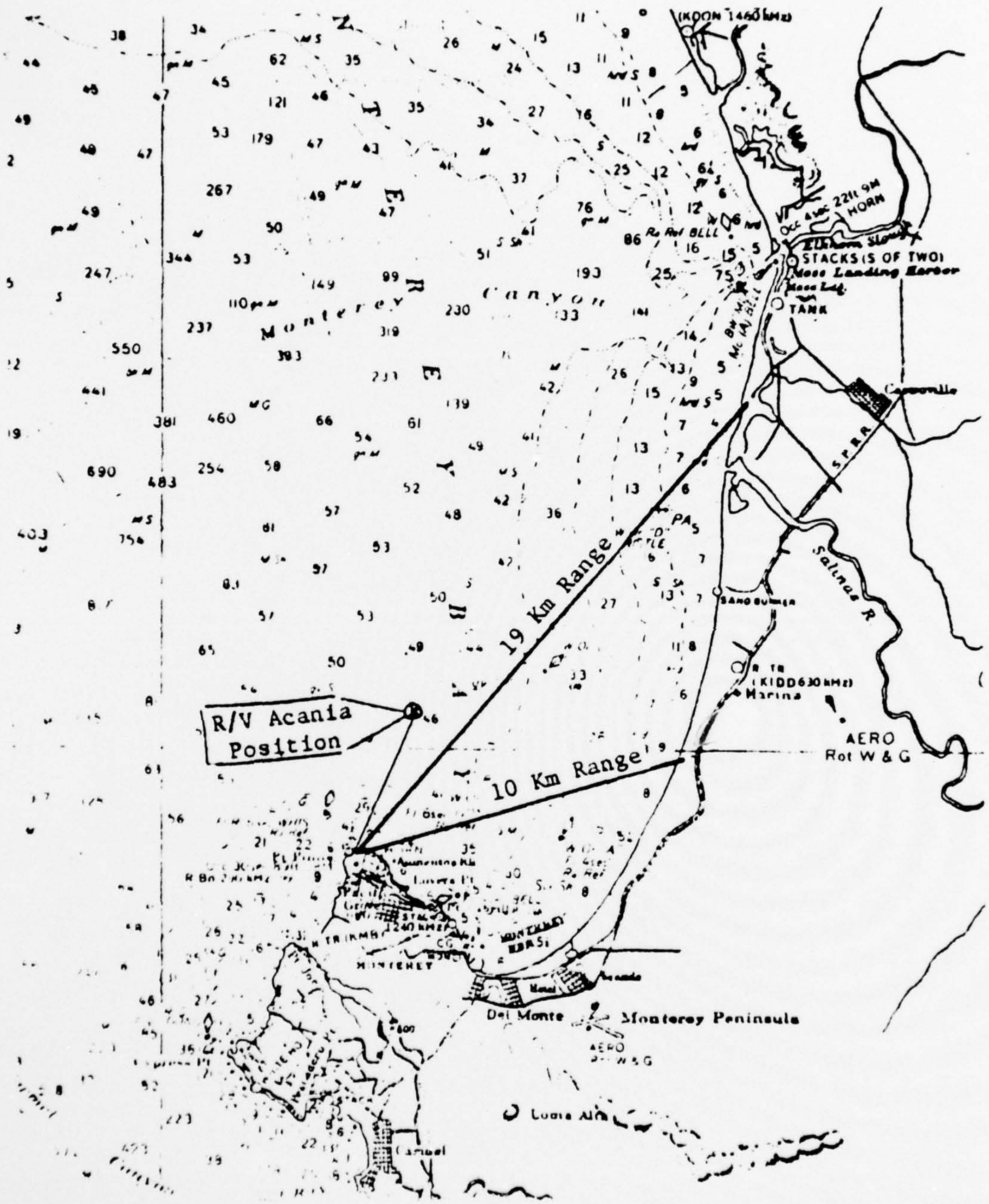

Figure 5.
Experimental site in Monterey Bay

is shallow enough that the ACANIA can anchor at any range up to about 15 km to the north and northeast.

B. INSTRUMENTATION

1. Wind-Temperature Measurement Systems

The mean wind measurements were made with a Thornthwaite Associates cup anemometer wind profile register system, model number 104. In operation the shaft of a three cup anemometer unit serves as the shutter between a light source and photocell for each revolution. The cups are plastic cones reinforced with aluminum frames. They are attached to the rotating shaft by stainless steel tubing spaced at 120 degree intervals about the shaft as shown in Figure (6). The three cup assembly sets along with the other sensors were positioned at four levels on the bow with electrical leads to the after deck house laboratory. The sets have the characteristics of low starting speeds with a small amount of internal friction which aids in checking inertial overshoot.

Temperature sensitive quartz crystal probes, (Hewlett Packard model HP-2850) were used to measure mean temperatures at each level. RF signals from the crystal probes and from a reference oscillator were mixed in the HP-2801A readout unit to produce a beat frequency whose signature can be

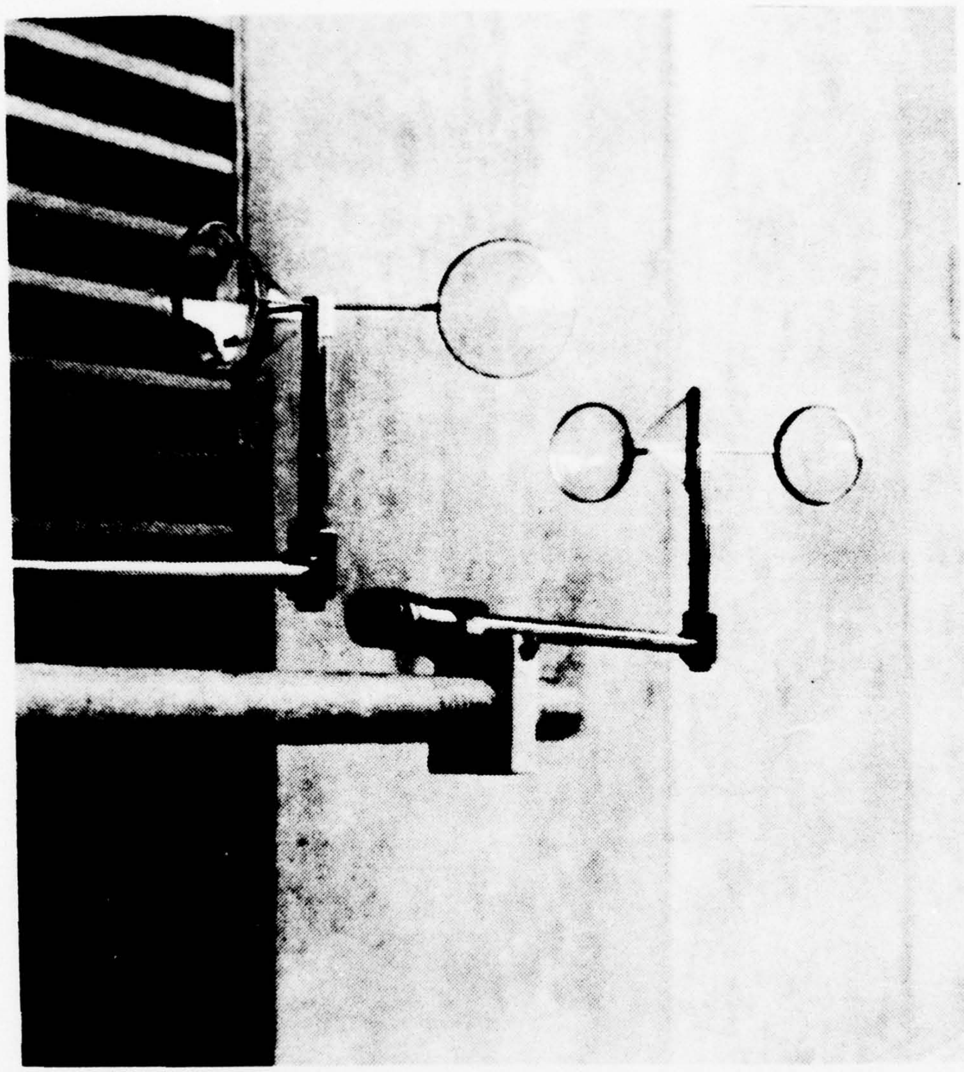

Figure 6.
C. W. Thornthwaite Anemometer Cups

analyzed to within 0.001 degrees centigrade per hertz. Each sensor simultaneously received pre-experiment calibration against a platinum resistance wire thermometer in a temperature controlled circulating water bath over the expected temperature range. The accuracy in achieving a 0.005 degree centigrade correction factor was a constant for each probe. A 3.7 meter flexible coaxial cable is permanently attached to the sensor head and the mast mounted probes are housed in an aspirated shelter as depicted in Figure (7). Temperature values were automatically recorded on a printer tape.

The temperature fluctuations were measured using a bridge developed by personnel at GTE Sylvania, the GTE Sylvania Model 140. The system was slightly modified for use in this study, and is described by Karch (1976).

2. <u>Humidity Measurement Systems</u>

To determine their accuracy and reproducibility, detailed examination in laboratory conditions has been made of the calibration characteristics of two humidity sensors, the Hygrodynamics Digital Hygrosensor and the Electro-Magnetic Research Corporation Lyman-alpha Sensor. These calibrations were based on ambient humidity variations (from 24% RH to 50% RH over a one month period), as measured with a Bendix Psychron Wet-Dry Bulb Psychrometer, and controlled humidity (from 40% RH to 99% RH) as measured by the

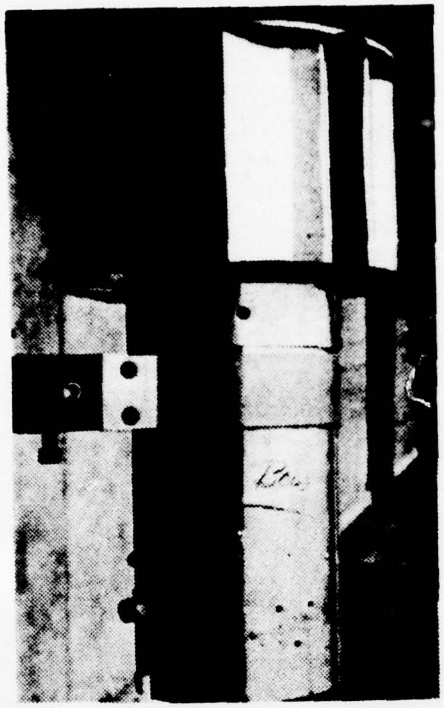

C.C. Breidert Company
Air-X-Houster Type 6L

Dunmore-type Lithium
Chloride Sensor

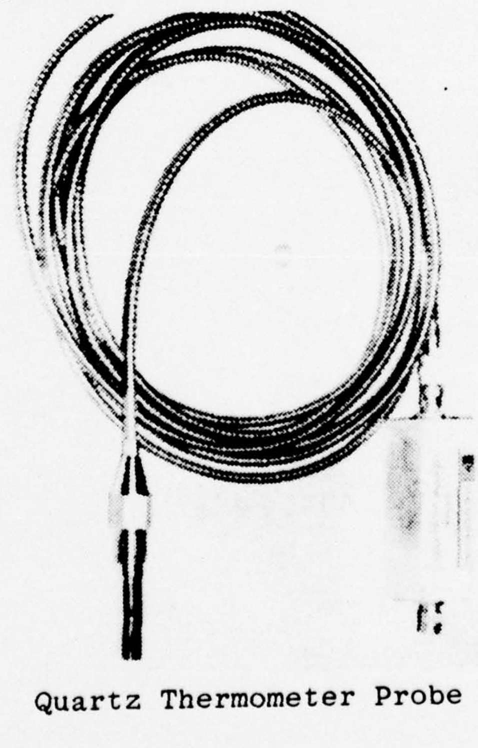

Quartz Thermometer Probe

Figure 7.
Photographs of aspirated shelter, hygrometer
and thermometer probe

wet-dry bulb thermocouple in a 2 x 3 x 3 ft. fog chamber adapted for these experiments. The air circulated through the chamber can be pre-humidified in a column of wet glass beads giving nominal humidity of about 80%. Higher humidities (up to 99% RH) can be obtained by introducing varying amounts of water in the form of a fine mist into the chamber. In general, the humidity in the chamber can be stabilized for periods of several hours and is uniform throughout the chamber to within 1% RH.

a. Hygrodynamics Digital Hygrosensor

The hygrosensor is a Dunmore-type lithium chloride sensor whose resistance varies in proportion to the relative humidity to which it is exposed. It is a slow-response sensor and is generally utilized in mean system measurements. The standard procedure of calibrating these sensors in a small chamber with a saturated salt solution of known vapor pressure was not satisfactory for a program of calibration of eight sensors. This dissatisfaction was primarily due to a lack of confidence in the ability to reproduce humidity conditions in consecutive sensor calibrations. Attempts to calibrate all eight sensors simultaneously in a large volume chamber were complicated by temperature drifts that made it difficult to assure equilibrium saturations necessary to the accuracy of the technique.

As a result of the above problems it was decided to use the humidity controlled chamber previously described. The quantitative results of their calibration are given in Table I; in general, the eight sensor average agrees with the psychrometer standard to -0.4 ± 2.9% RH for measurements taken with equilibrium times of order one hour. The individual total humidity accuracy of the sensor is of less importance that the relative consistency within the group of sensors, since we use them in a four-level system to determine the humidity gradients. In this respect, they can be calibrated to ± 1% RH, subject to assurances of sufficient time for response.

The suitability of the hygrosensors for shipboard measurement of humidity gradients is reduced by two inherent properties of the device. An aspirated, teflon-coated sensor has a time constant of about 30 minutes, but this varies from sensor to sensor. Therefore, the humidity difference read between two sensors will be unreliable if the humidity is changing faster than about 10% RH per half-hour. A more serious deficiency appears if the sensors are exposed to humidities about 95% RH. At those high humidities, the sensors become sluggish and exposure to 99% RH may cause the sensors to be useless for as long as several days.

TABLE I

Hygrodynamics Digital II Calibration

Wet-Dry Bulb %RH	Ave Hygro %RH	Deviation of Sensor from Ave Hygro % RH 1	2	3	4	5	6	7	8
33.	3.16	1.4	-1.4	-0.6	1.5	-0.2	-1.6	-0.9	1.8
36.	37.2	-0.5	-0.8	-0.3	1.6	0.5	-1.4	-0.1	1.2
44.	41.2	-0.8	-0.4	-0.3	0.6	0.9	0.4	-0.1	0.3
NA	41.5	-0.5	-0.4	-0.3	0.5	0.9	-0.4	-0.1	-0.1
NA	42.6	-1.2	-0.5	-0.5	-0.9	1.8	-0.4	-0.2	0.1
NA	65.8	-0.2	-1.4	-2.5	0.8	1.8	-0.3	1.3	0.3
74.8	73.6	0.2	0.2	-1.3	0.5	-0.2	0.4	-0.4	0.8
88.3	85.0	-0.7	0.9	-0.4	0.1	-0.6	0.0	0.4	0.2
82.6	86.7	-1.4	-0.6	-0.5	0.1	-0.2	0.3	0.7	0.3
82.6	87.0	-1.0	0.5	-0.7	0.0	0.3	0.7	0.0	0.2
85.0	88.0	-0.4	1.1	-0.1	0.1	-1.8	1.1	-0.6	-0.1
93.9	89.6	0.1	0.8	-0.2	0.3	-2.2	2.1	-1.5	0.4
94.4	92.3	-0.6	1.1	-0.5	-0.3	-0.4	1.2	-0.5	0.4
94.4	93.6	-0.8	1.0	-0.8	-0.3	0.4	-0.2	0.8	-0.4
Ave Deviat		-0.5	-0.0	-0.6	0.3	0.1	0.1	-0.1	0.4
		0.7	0.9	0.6	0.7	1.1	1.0	0.7	0.6

The average deviation of the wet-dry bulb from the Ave Hygro reading is 0.4% RH with a standard deviation of 2.9% RH.

b. Electro-Magnetic Research Corporation
Lyman-alpha Sensor

The Lyman-alpha sensor measures humidity as a function of the absorption of ultraviolet light by the Model 1215Å Lyman-alpha transition of hydrogen in water vapor. It consists simply of a UV source tube and detector, separated by an absorbing air gap.

The detector voltage is proportional to the total light transmitted and is related to the absolute humidity, q (in mb), by the equation

$$V = V_o \exp(-\lambda q) \tag{24}$$

The Lyman-alpha is a fast response device and is specifically used for measurement of humidity fluctuations, q'. Eqn (24) can be manipulated to relate q' to voltage fluctuations V', giving

$$q' = -\frac{1}{\lambda}\frac{V'}{V} \tag{25}$$

The quantity V_o in Eqn (24) is the sensor output voltage in dry air which can be found by placing the detector in dehumidified air.

Because water soluble windows (LiF or MgF_2) are required for transmission in the ultraviolet, V_o is a highly variable quantity, a property which makes the Lyman-alpha a

poor device for measurement of total humidity, q. However, Eqn (25) shows that the fluctuating part, q', depends only on λ , which is a property of water vapor and the gap setting only and is independent of the window condition so that q' can be reliably measured. The Lyman-alpha has been calibrated in dry air, ambient air, and in a humidity chamber and it was found that $\lambda = .225\ mb^{-1}$ for a source current = 50 μa and a 1 cm air gap. The calibration curve appears in Figure (8).

The feasibility of the Lyman-alpha sensor for shipboard humidity fluctuation measurements is subject to considerations of the survivability of the windows in the ocean environment of high humidity, sea spray, and rain. In the laboratory humidity chamber, it was observed that V_o would decrease by a factor of four after a three-day exposure to 85% humidity. Consequently, it will be necessary to provide better physical protection for the sensors during routine operations.

3. Data Recording

All mean data recorded for this study was logged using an NPS developed micro-processor based data acquisition system, the MIDAS (Microprogrammable Integrated Data Acquisition System). It is fully described by Atkinson (1976). In this study a ten minute averaging period was

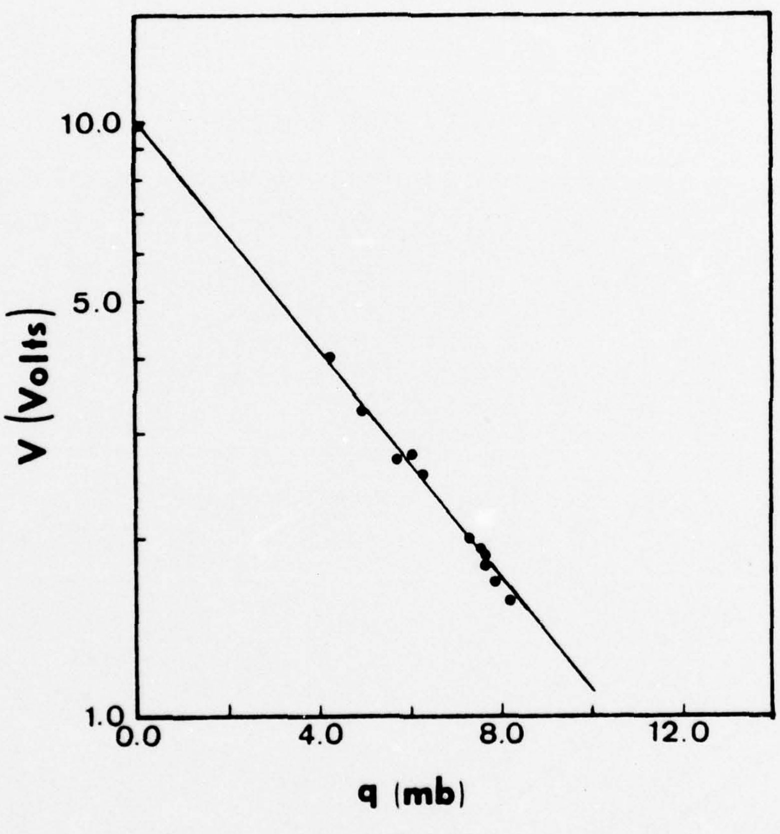

Figure 8.
Calibration graph of Lyman-alpha humidiometer

used to define the mean data. Temperature, relative humidity, and mean wind data was punched on paper tape by the MIDAS unit; the data was later transferred to computer cards for further analysis.

Voltage signals corresponding to measured fluctuating humidity, q', were recorded on magnetic tape using a Sanborn Model 3950 fourteen channel tape recorder. In addition, the average voltage output of the Lyman-alpha sensor was recorded on a brush type chart recorder. The latter was necessary to define V in the voltage to humidity conversion expression, Eqn (25).

C. ANALYSIS PROCEDURES

Data analysis was carried out for data collected during a four day cruise in April 1976. Mean data was obtained for each of the four levels during the entire cruise. However, only two Lyman-alpha humidiometers were available so q' data was collected at only two levels. These two instruments were placed at levels 6.6 and 13.9 meters above mean water level. Due to the failure of a source tube in the instrument at the upper level, q' data was available from only the 6.6 meter level. Table II summarizes periods examined and data available for each period.

TABLE II

Summary of Data Periods

Date 1976	Time	Number of Levels $\overline{q}/q'$	Number of Profiles/Spectra $\overline{q}/q'$
27 April	1446-1930	4/1	12/6
28 April	1320-1939	4/1	33/24
29 April	1410-2240	4/1	42/24
30 April	1033-1138	4/1	21/13

All data were first edited for gross errors or inconsistencies due to equipment malfunctions. The criterion at this point for retaining or rejecting data periods depended on whether C_q^2 values could be computed from humidity spectra for the time periods involved.

Lyman-alpha data were analyzed on the basis of the strip charts to give an average voltage output at ten minute intervals. Relative humidity data from the MIDAS output was converted to specific humidity $\overline{q}$, by use of the governing meteorlogical equations for moist air. Virtual potential temperatures, Θv, were calculated using IBM 360 routines. The values of $\overline{q}$ and Θv were then plotted versus the logarithm of height. Best fit lines were drawn to the points from

which slopes were picked off and applied to the expressions developed by Wyngaard et al.

1. Profile Analyses

Virtual potential temperature, Θv, and specific humidity, $\overline{q}$, values were plotted on semi-logarithmic paper, since Θv, and $\overline{q}$ are parameters which vary logarithmically with height. A best fit straight line was then drawn to the data points. The procedures, of course, were subjective, and in many instances several different slopes could be obtained from just one graph. Hence a criterion used was not to give single data points too much weight in determining the best fit line. Consequently, the line drawn represented a most probable position between data points as illustrated in Figure (9).

Difficulty arose whenever anomalous points appeared in a graph as in Figure (10) where the specific humidity at the second level was obviously inconsistent with the other three levels. In a case such as this, the inconsistent point was merely ignored.

2. $C_q^{\ 2}$ Analysis Procedures

Analog spectral analyses procedures were applied to the humidity fluctuation data to obtain variance spectrum. Appropriate 21 minute segments of data recorded on magnetic tape were recorded into an EMR-Schlumberger Model 1510

(a)

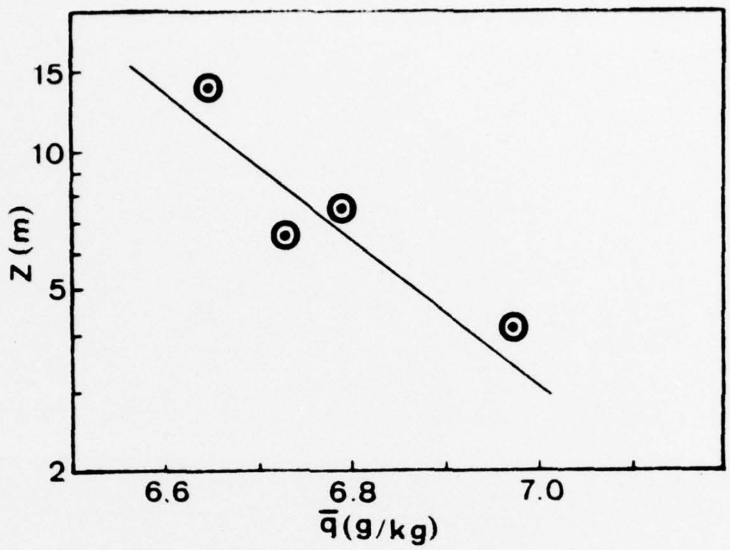

(b)

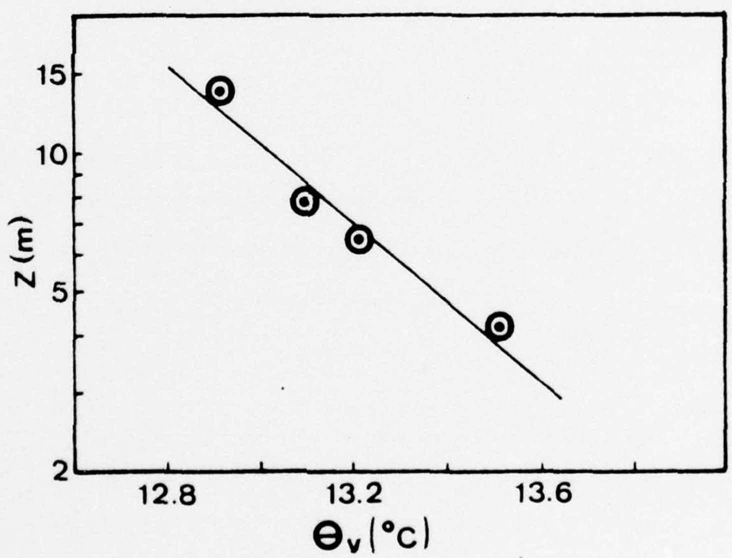

Figure 9.
Typical profiles for
a) specific humidity - 30 April 76 (1210)
b) virtual potential temperature - 29 April 76 (1052)

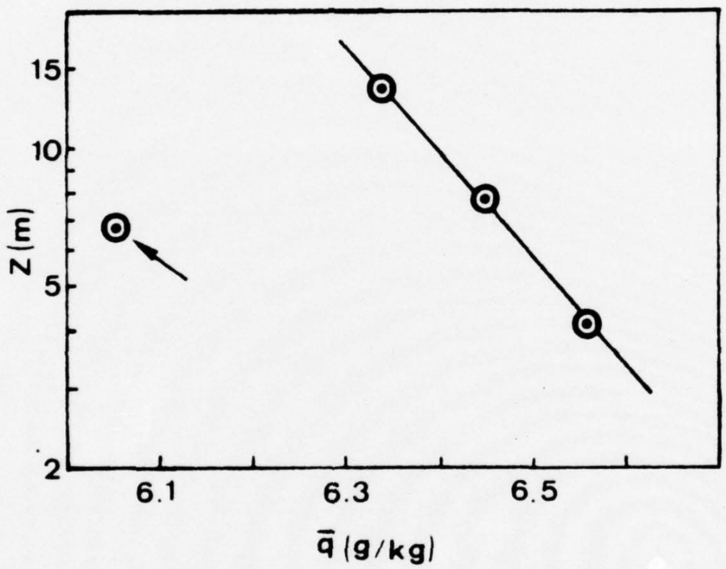

Figure 10.
Profile of 27 April 76 (1817) showing an anomalous specific humidity reading at the 6.6 meter level.

Digital Spectrum Analyzer. The procedures required to convert spectral values, obtained with the digital spectrum analyzer, to engineering units and then to obtain ${C_q}^2$ values from appropriate spectra are described in the following subsection. A parallel discussion for temperature spectra appears in Hughes (1976).

a. Scaling Spectral Plots

A necessary procedure was to scale the spectral plots to relate RMS input voltages to power spectral densities (PSD); variance per unit frequency. To obtain power spectral density levels, corresponding to RMS voltage inputs, calibrated scale charts had to be constructed.

For purposes of the x-y plot format of the analyzer output, the RMS voltages were converted to $y=\log_{10}$ (voltage) units and a graduated scale was constructed so that the logarithm of volts RMS could be interpolated from spectral plots. The value of the vertical scale (y) was adjusted for each spectrum as a function of both input gain and spectral gain. These values were then converted to PSD levels for use in calculating ${C_q}^2$ values.

The relation between Volts RMS to PSD units used was

$$S(f)\ \{\underline{\text{PSD}}\text{ units}\} = \frac{(\text{cal. level VRMS})^2}{1.5\text{ Bandwidth}} \times (10^y)^2 \quad (26)$$

where Bandwidth = $\frac{\text{Freq. Range}}{\text{No. Channels}}$

$$\left(= \frac{256 \text{ Hz}}{256} = 1 \text{ Hz} \right)$$

and cal. level Vrms = voltage at y=0

(= 1 Vrms for 3.16 V input setting).

Amplitude scaling calibrations were accomplished using externally generated "white noise" signals of 1 Volt RMS with a frequency range from 0.1 Hz to 1000 Hz (giving a PSD of $10^{-3}V^2$/Hz). Setting a 3.16 V (10dB) input on the EMR 1510 Digital Spectrum analyzer insures that 1 Volt corresponds to y=0. An example of such a calibration plot for a frequency range of 1-200 Hz (the frequency range of interest) is shown in Figure (11).

b. Computation of Turbulence Parameters from Scaled Spectra

Values of the turbulence parameter C_q^2 were obtained from the humidity variance spectra on the basis of the formula for the inertial subrange in wave number space S(k), Eqn (1), which predicts a -5/3 slope for the spectra when plotted in a log-log format. Figures (12), (13), and (14) are typical spectra considered in the analyses. Humidity spectra often exhibited slopes slightly different than the expected -5/3, except in the frequency

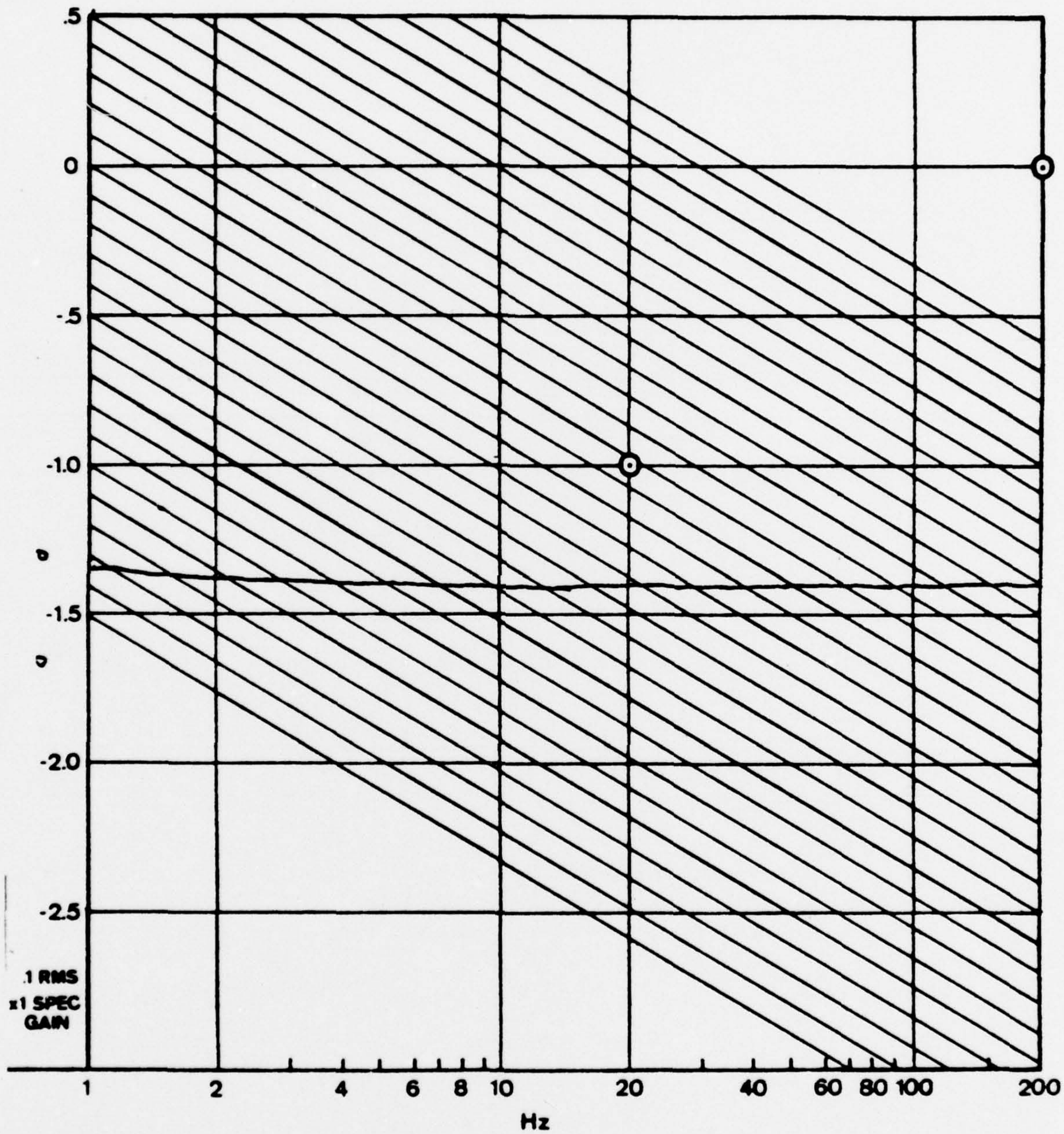

Figure 11.
Calibration plot for spectrum analyzer

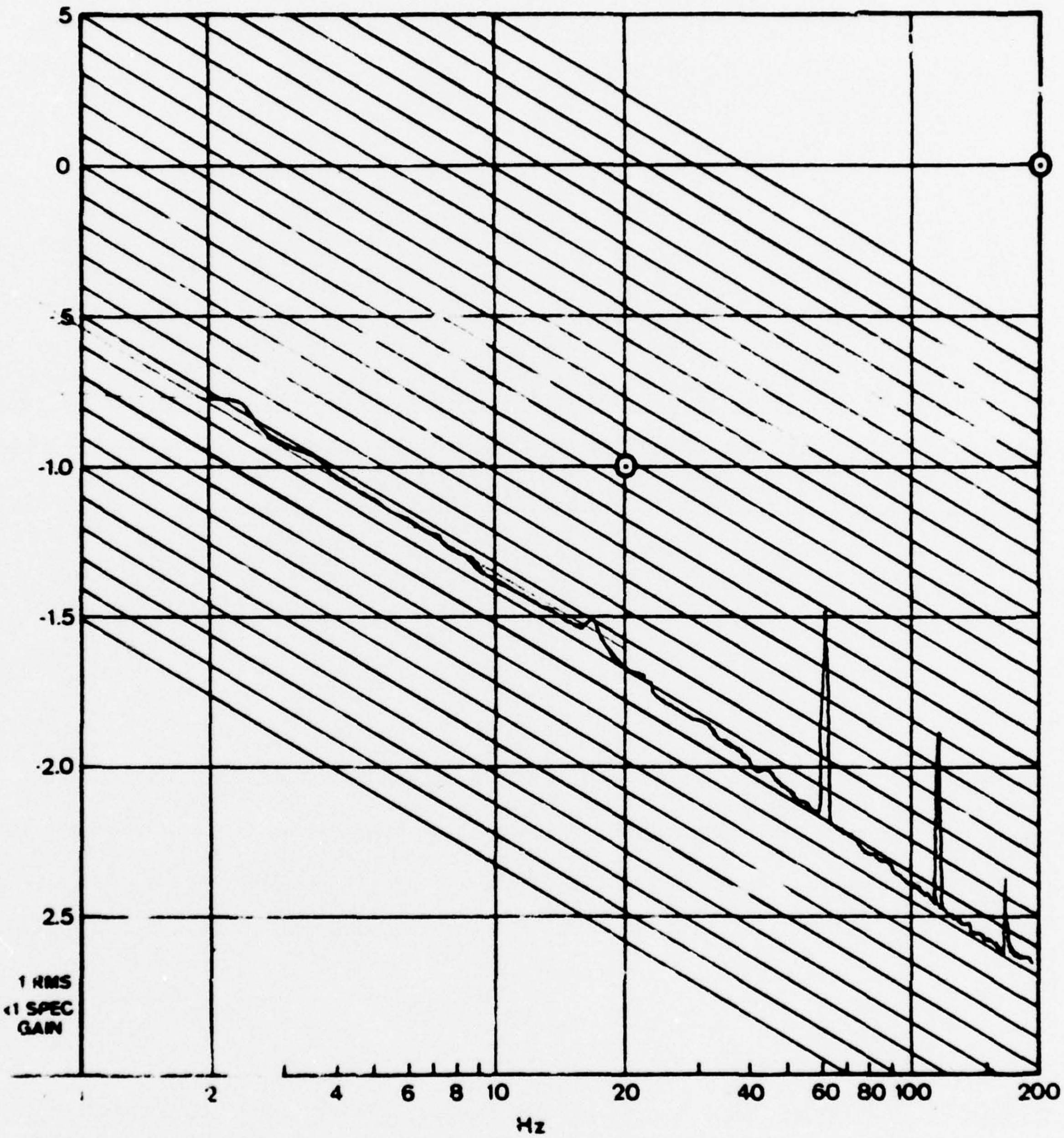

Figure 12.
Typical humidity spectra showing -5/3 slope in the range from 1 Hz to 10 Hz

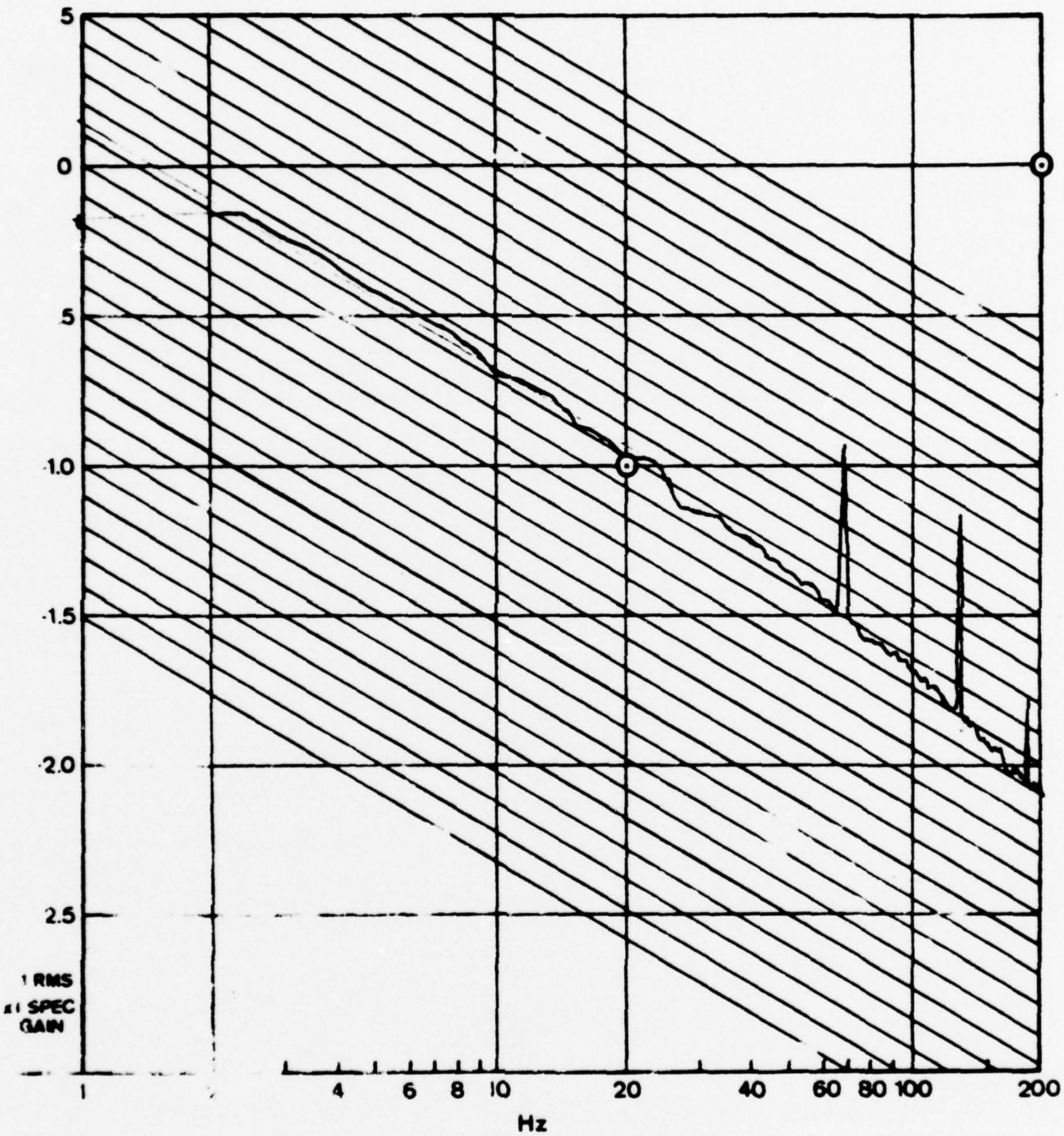

Figure 13.
Typical humidity spectra showing -5/3 slope in the range from 1 Hz to 10 Hz

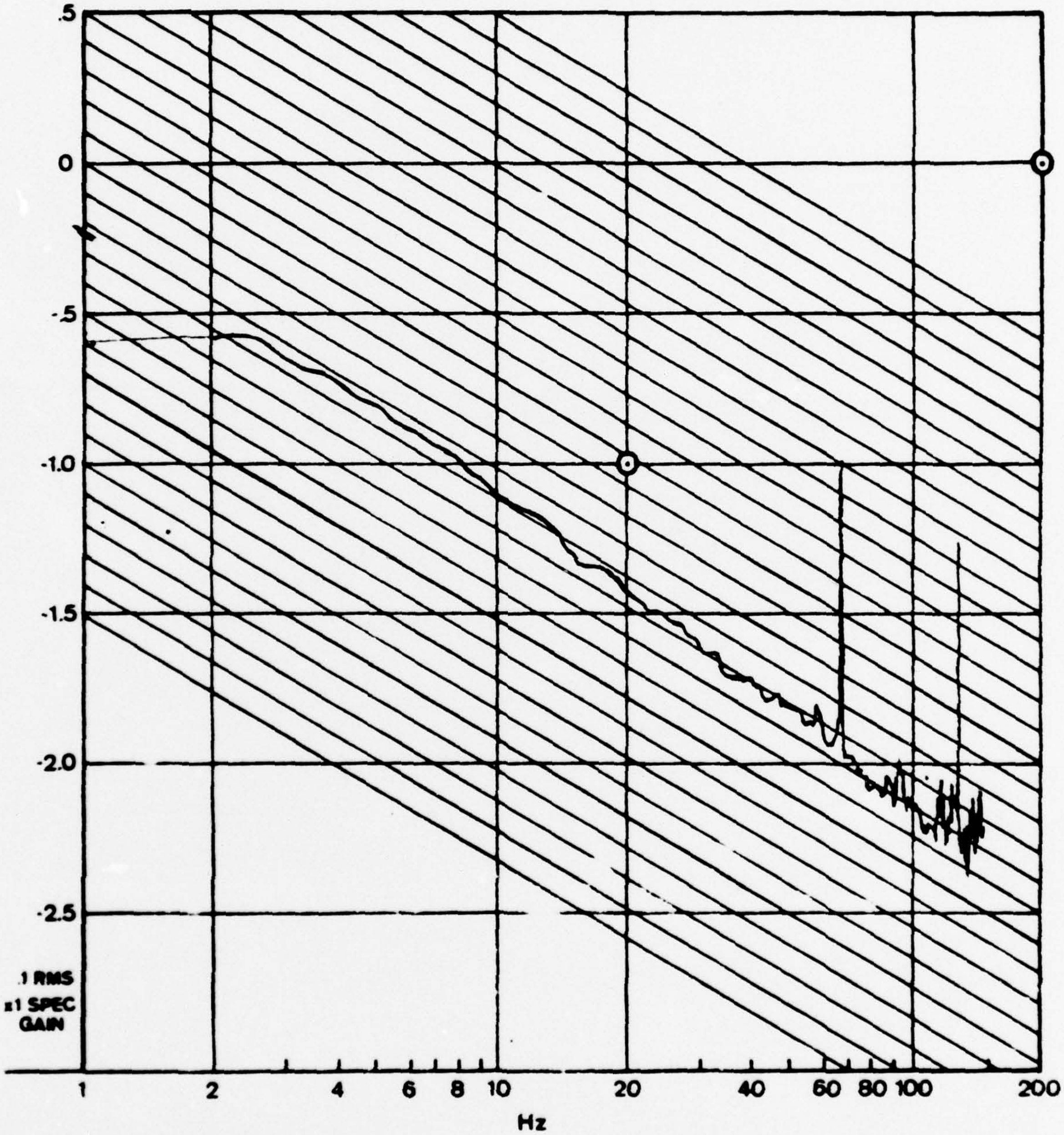

Figure 14.
Typical humidity spectra showing -5/3 slope in the range from 1 Hz to 10 Hz

range of 1 Hz to 10 Hz. This feature of humidity spectra has been observed by others, namely Friehe (1975). A universally accepted explanation has not been postulated to account for this phenomena. Figure (15) is an example of a spectra which does not exhibit a -5/3 slope in any frequency range. Approximately 10% of spectra studies fell into this category.

Assuming -5/3 slopes for the variance spectra, the intercept of the best fit -5/3 slope with the 1 Hz frequency line was the spectral density denoted (PSD) value used to compute C_q^2. The measured PSD value was converted to engineering spectral density units by the relation

$$\begin{aligned} S_q(f) &= C_{L-\alpha}^2 \cdot \mathrm{PSD} \\ &= (\mathrm{g/kg/Volt})^2 \cdot \mathrm{Volt}^2/\mathrm{Hz} = (\mathrm{g/kg})^2/\mathrm{Hz} \end{aligned} \tag{27}$$

where $C_{L-\alpha}$ was the calibration factor for the Lyman-alpha humidiometer.

Since the humidity fluctuations were measured at a fixed point in the flow, the resultant spectral values are defined at "temporal" frequencies denoted as $S_q(f)$ in Eqn (28). In order to obtain C_q^2 from Eqn (6) temporal (f) and space (k) scales had to be related. This was accomplished by using Taylor's "frozen turbulence" hypothesis discussed

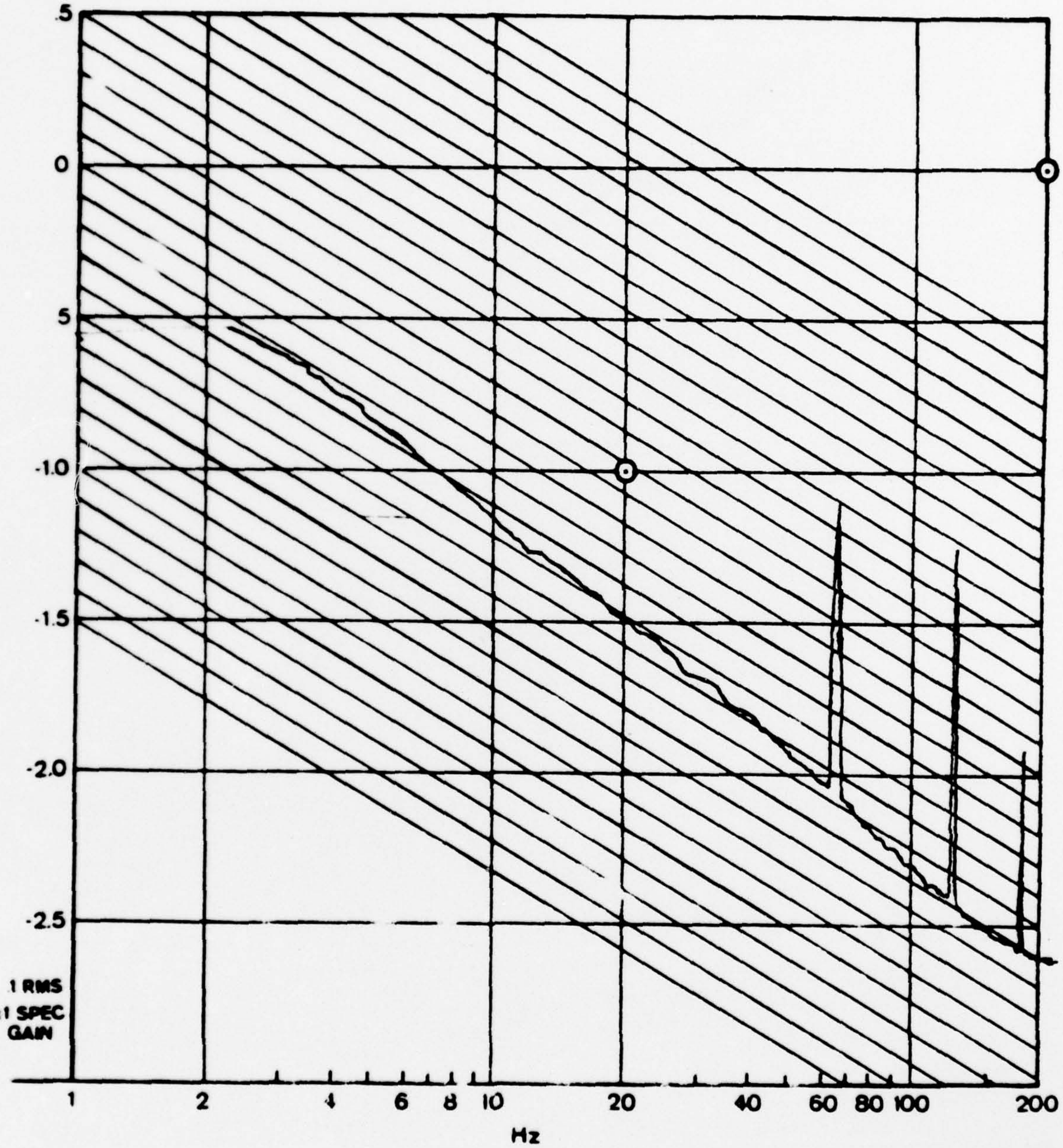

Figure 15.
Humidity spectra lacking a distinct -5/3 slope

in section II.B. The following equation relates temporal to wavenumber variance spectral values,

$$fS_q(f) = kS_q(k) = c_2 C_q^{\,2} k^{-2/3} \tag{28}$$

where $S_q(f)$ is the spectral density value with units of $(g/kg)^2/Hz$.

Eqn (28) leads to the following relationship between $C_q^{\,2}$ and $S_q(f)$,

$$C_q^{\,2} = \frac{k^{2/3}}{c_2} fS_q(f) \tag{29}$$

where, $c_2 = 0.25$, an empirical constant, and $k = 2\pi f/\overline{U}$. Hence, with measured values of f, $S_q(f)$, and $\overline{U}$, $C_q^{\,2}$ was then determined from Eqn (29) for the level of interest, z.

3. Procedures to Calculate Vertical Humidity Flux

Vertical humidity flux $(\overline{w'q'})$ was calculated using two different methods; one utilized the spectrally derived $C_q^{\,2}$ values, and the other utilized the profile of mean humidity. The results were compared on a linear plot to determine if any relationship could be observed.

a. The Spectral Method

This method of calculating $(\overline{w'q'})$ was based on $C_q^{\,2}$ values derived from variance spectra of the Lyman-alpha humidiometer using Eqn (18). In this calculation the values

of ϵ which were used were derived from wind fluctuation data by Karch (1976).

b. The Profile Method

This method utilized the vertical gradient of mean humidity and the friction velocity, U_*, to calculate $(\overline{w'q'})$ from Eqn (23). The profiles of $\overline{q}$ were evaluated and values of $\overline{q}$ were read off at two different levels from the best fit line drawn to all but erroneous points.

The values of U_* used in these computations were determined from the ϵ values obtained by Karch (1976). The final relation used was

$$U_* = (\epsilon \kappa z)^{1/3} , \qquad (30)$$

which appears to give the most consistent estimates for U_* in the marine boundary layer.

IV. RESULTS

Observed humidity index-structure parameter results, made non-dimensional according to the Wyngaard et al prediction, Eqn (16), appears in Figure (16). In the figure individual data points appear as dots, and averages over Ri intervals of 0.25 appear as dots within a larger circle. The error bars are standard deviations from the mean within each interval, while the number at the top of the error bars is the number of observations defining the mean value. For both the stable (+Ri) and unstable (-Ri) stratification cases, there appears to be little agreement and no definite trends.

Scatter in the observed results in Figure (16) can be attributed to scatter in both the measured $C_q^{\ 2}$ values as well as $\partial \overline{q} / \partial z$ values. Deviation of humidity spectra from a -5/3 slope also caused uncertainty in $C_q^{\ 2}$ estimates.

The values for $\partial \overline{q} / \partial z$ are important because the humidity gradients were, in most cases, small, and enter into the normalization of $C_q^{\ 2}$ as a squared value.

Significantly, non-dimensional $C_q^{\ 2}$ results obtained in this study were generally an order of magnitude smaller than $C_T^{\ 2}$ results obtained by Wyngaard et al (1971) and

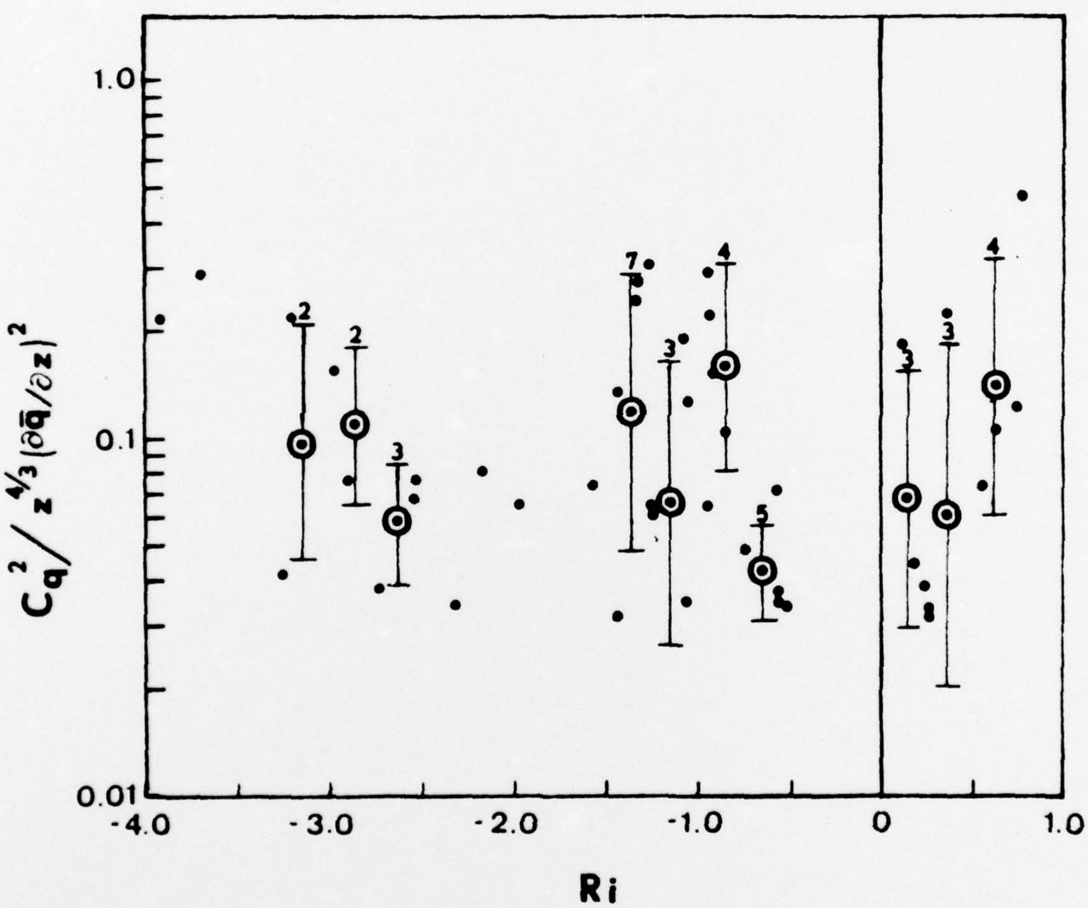

Figure 16
Results of the spectrally derived humidity-structure parameter vs. the Richardson Number

and Hughes (1976). All sensors, calibrations, and governing equations were rechecked. All calculations were redone. However, the final results remained smaller in value than expected. It was expected that results would fall in the same order of magnitude as C_T^2 since both temperature and humidity are scalars. One possible explanation is that the value of β from Eqn (1) is not the same for both temperature and humidity, as presently postulated.

If the scatter of the non-dimensional C_q^2 values is ignored, the results can be seen to be essentially constant. If one is willing to accept the error of an order of magnitude, then given a gradient of $\overline{q}$ and a height z, C_q^2 can be computed according to the expression

$$C_q^2 = z^{4/3} \left(\partial \overline{q} / \partial z \right)^2 \tag{31}$$

The comparison of the vertical humidity flux calculations appear in Figure (17). $(\overline{w'q'})$ obtained from C_q^2 data are denoted $(w'q')_{L-\alpha}$ and vertical humidity flux obtained from profiles of $\partial \overline{q} / \partial z$ are denoted $(\overline{w'q'})_P$. There is no observed correlation between the two values. Perhaps new dimensionalizing parameters need to be developed in order to be able to predict values of $(\overline{w'q'})$ accurately.

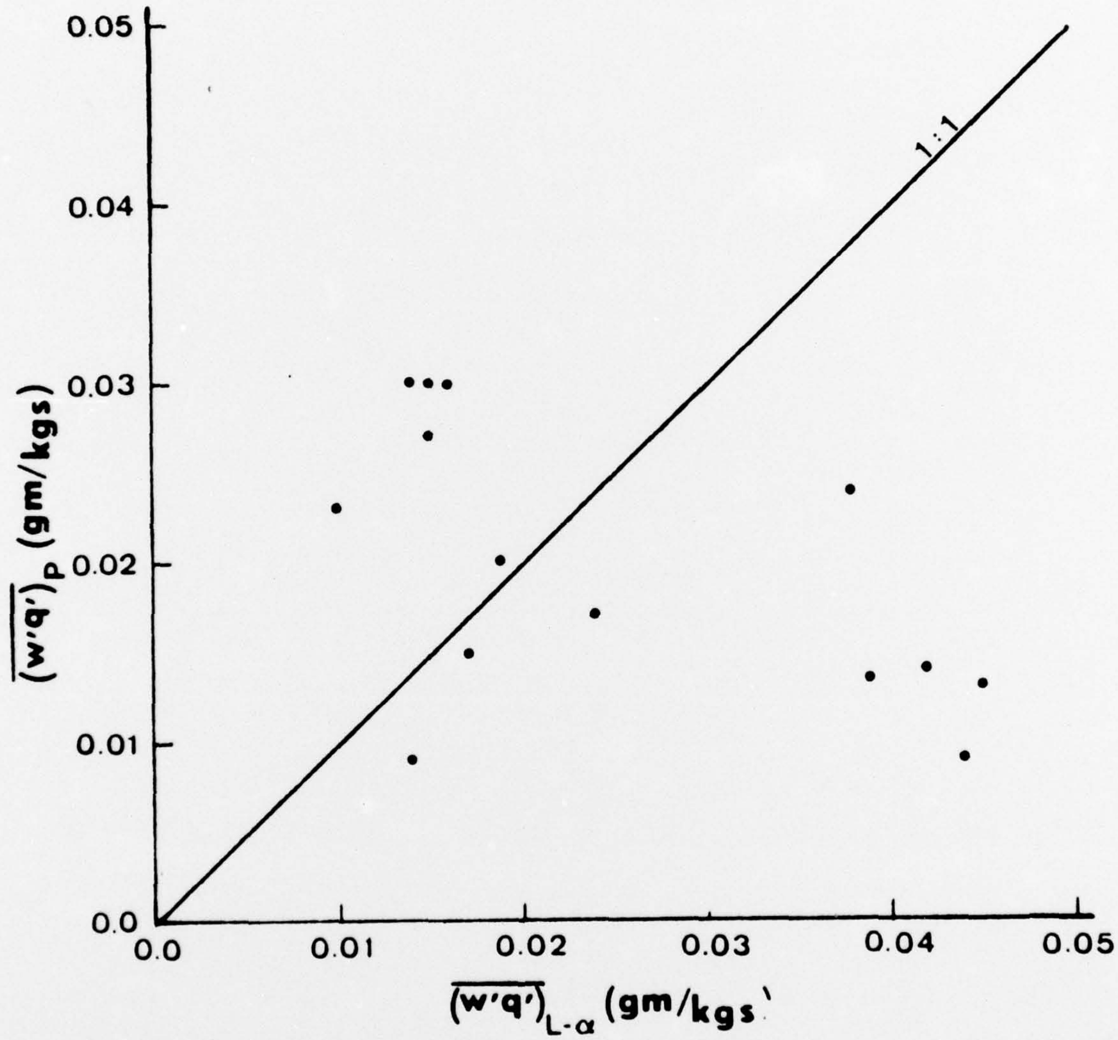

Figure 17.
Results of the comparison between vertical humidity flux calculated by the profile method, $\overline{(w'q')}_P$, vs. the vertical humidity flux calculated using C_q^2 values, $\overline{(w'q')}_{L-\alpha}$

Table III summarizes data used to construct Figure (16). Tables IV and V contain values used in the comparison shown in Figure (17). Values in all three tables were computed at the 6.6 meter level.

TABLE III

C_q^2 and Ri Results

Time	$\overline{U}$	$\partial\overline{q}/\partial z$	$C_q^2 \times 10^{-3}$	Ri
27 April				
1446-1509	7.70	-0.043	1.48	-1.26
1509-1520	8.17	-0.045	0.88	-1.07
1520-1540	7.84	-0.048	0.92	-1.44
1540-1600	7.50	-0.037	1.08	-1.27
1620-1640	6.25	-0.045	0.96	-2.73
1910-1930	4.03	-0.030	1.72	-0.90
28 April				
1320-1337	5.16		2.60	
1337-1355	5.30	-0.026	2.04	-1.32
1355-1413	5.16	-0.025	1.72	-0.93
1415-1420	5.06	-0.028	1.24	-1.05
1433-1451	5.02	-0.024	1.96	-1.32
1452-1504	4.39	-0.024	2.08	-0.95
1511-1517	4.88	-0.023	2.00	-1.26
1526-1533	4.50	-0.031	1.84	-2.96
1540-1551	4.31	-0.031	2.60	-3.20
1556-1606	4.40	-0.024	2.05	-3.70
1613-1621	5.30	-0.032	1.67	-1.42
1633-1641	4.97	-0.039	1.52	-2.19
1652-1701	4.73	-0.038	1.27	-0.58
1720-1738	4.31	-0.044	1.09	0.19
1739-1744	4.03	-0.051	1.56	-0.74
1757-1807	4.31	-0.048	1.00	-0.58
1807-1817	4.31	-0.053	1.29	-0.58
1817-1827	4.08	-0.057	1.36	-0.52
1827-1837	4.03	-0.052	1.32	0.24
1837-1847	3.91	-0.052	1.07	0.29
1847-1857	3.61	-0.053	1.16	0.29
1909-1919	2.80	-0.045	1.72	1.68
1919-1929	2.50	-0.033	1.51	7.01
1929-1939	2.50	-0.028	1.60	7.89
29 April				
1410-1420	5.88	-0.020	2.36	0.79
1420-1430	5.86	-0.039	3.36	0.12
1442-1452	5.86		6.40	
1500-1513	6.43		3.45	

Table III Continued

Time	$\overline{U}$	$\partial \overline{q} / \partial z$	$C_q^2 \times 10^{-3}$	Ri
1521-1532	6.00		3.10	
1541-1553	4.50		3.77	
1600-1610	5.86		2.51	
1653-1703	4.26	-0.039	2.36	-6.15
1703-1713	4.92	-0.024	1.72	-4.06
1713-1723	4.31	-0.023	1.68	-10.94
1723-1733	4.22	-0.014	1.71	-5.17
1733-1743	4.26	-0.011	2.60	-4.82
1830-1848	2.60		2.28	
1848-1906	3.61		2.41	
1916-1934	2.71		2.00	
1934-1952	2.83		2.16	
2000-2018	2.95			
2018-2036	3.36			
2036-2054	3.76		1.27	
2054-2114	3.81		1.25	
2125-2145	3.66		1.40	
2145-2157	3.76		1.60	
2203-2223	3.76		1.69	
2221-2240	4.71		1.60	
30 April				
1033-1043	4.73	-0.047	2.04	-1.56
1043-1053	4.45	-0.043	1.55	-2.52
1053-1103	4.31	-0.030	2.44	-3.91
1108-1118	4.40	-0.043	1.76	-2.90
1118-1128	4.55	-0.043	1.75	-2.52
1128-1139	4.78	-0.033	3.00	0.37
1148-1206	5.53	-0.031	1.44	0.74
1206-1224	5.53	-0.036	1.65	0.62
1224-1242	6.05	-0.054	1.04	0.0
1242-1250	4.40	-0.041	1.52	0.56
1250-1308	3.26	-0.034	1.83	0.0
1310-1328	3.41	-0.040	1.32	-1.98
1328-1346	3.51	-0.032	0.83	-0.96

TABLE IV

$\overline{w'q'}$ Results, $C_q^{\ 2}$ Method

Time	$\epsilon\,(x10^{-3})$	$C_q^{\ 2}(x10^{-3})$	$\partial\overline{q}/\partial z$	$\overline{w'q'}$
28 Apr 76				
1337-1355	2.90	2.04	-0.026	0.045
1355-1413	3.67	1.72	-0.025	0.042
1757-1807	4.55	1.00	-0.048	0.014
1807-1817	4.60	1.28	-0.053	0.016
1817-1827	4.66	1.36	-0.057	0.016
1827-1837	4.76	1.32	-0.052	0.017
1837-1847	4.95	1.16	-0.053	0.015
29 Apr 76				
1653-1703	4.00	2.36	-0.039	0.038
1703-1713	3.50	1.72	-0.024	0.044
1713-1723	2.33	1.68	-0.023	0.039
1723-1733	2.80	1.72	-0.014	0.069
1733-1743	3.04	2.60	-0.011	0.014
30 Apr 76				
1033-1043	0.97	2.04	-0.047	0.017
1224-1242	2.09	1.04	-0.054	0.010
1242-1250	2.09	1.52	-0.041	0.019
1250-1308	1.37	1.84	-0.034	0.024

TABLE V

$\overline{w'q'}$ Results, Profile Method

Time	$q(z_2)-q(z_1)$	U_*	$\overline{w'q'}$
28 Apr 76			
1337-1355	6.15-6.18	0.19	0.013
1355-1413	6.27-6.30	0.20	0.014
1757-1807	6.77-6.83	0.22	0.030
1817-1827	6.78-6.84	0.22	0.030
1827-1837	6.79-6.85	0.22	0.030
1837-1847	6.82-6.87	0.23	0.027
29 Apr 76			
1653-1703	6.30-6.35	0.21	0.024
1703-1713	6.41-6.43	0.20	0.009
1713-1723	6.39-6.42	0.18	0.013
1723-1733	6.33-6.35	0.19	0.009
1733-1743	6.40-6.42	0.19	0.009
30 Apr 76			
1033-1043	6.62-6.67	0.13	0.015
1224-1242	7.11-7.17	0.17	0.023
1242-1250	7.12-7.17	0.17	0.020
1250-1308	7.08-7.13	0.15	0.017

LIST OF REFERENCES

1. Atkinson, H. E., III (1976): Turbulent Flux Estimates from Shipboard Mean Wind and Temperature Profiles and Dissipation Rates, M.S. Thesis, Naval Postgraduate School, Monterey, California, 66 pp.

2. Corrsin, S., (1951): "On the Spectrum of Isotropic Temperature Fluctuations in an Isotropic Turbulence," J. Appl. Phys., 22, 469-473.

3. Dyer, A. J. and Hicks, B. B. (1970): "Flus Gradient Relationships in the Constant Flux Layer," Quart. J. R. Met. Soc., 96, 715-721.

4. Friehe, C. A., La Rue, J. C., Champagne, R. H., Gibson, C. H., and Dryer, G. F. (1975): "Effects of Temperature and Humidity Fluctuations on the Optical Refractive Index in the Marine Boundary Layer," J. Opt. Soc. Am., 65, 1502-1511.

5. Hughes, M. M. (1976): An Investigation of Optically Relevant Turbulence Parameters in the Marine Boundary Layer, M.S. Thesis, Naval Postgraduate School, Monterey, California, 66 pp.

6. McBean, G. A. (1971): "The Variations of the Statistics of Wind, Temperature, and Humidity Fluctuations with Stability," Boundary-Layer Meterology, 1, 438-457.

7. McIntosh, D. H. and Thom, A. S. (1972): Essentials of Meteorology, Wykeham Publications Ltd., London, 239 pp.

8. Smedman-Hogstrom, A. (1973): "Temperature and Humidity Spectra in the Atmospheric Surface Layer," Boundary Layer Meteorology, 3, 329-347.

9. Taylor, G. I. (1938): "The Spectrum of Turbulence," Proc. Roy. Soc., 164, 476-490.

10. Wyngaard, J. C., Izumi, Y., and Collins, S. A. (1971): "Behavior of the Refractive Index Structure Parameter Near the Ground," J. Opt. Soc. Am., 61, 1646-1650.

INITIAL DISTRIBUTION LIST

		No. Copies
1.	Defense Documentation Center Cameron Station Alexandria, Virginia 22314	2
2.	Library, Code 0212 Naval Postgraduate School Monterey, California 93940	2
3.	Naval Oceanographic Office Library (Code 3330) Washington, D. C. 20373	1
4.	Director, Naval Oceanography and Meteorology NSTL Bay St. Louis, Mississippi 39520	1
5.	Prof. Kenneth L. Davidson, Code 51Ds Department of Meteorology Naval Postgraduate School Monterey, California 93940	9
6.	Prof. Thomas M. Houlihan, Code 59Hm Department of Mechanical Engineering Naval Postgraduate School Monterey, California 93940	2
7.	Dr. B. Katz, Code 213 Naval Surface Weapons Center White Oak Silver Spring, Maryland 20910	1
8.	Mr. Steve Rinard Department of Meteorology Naval Postgraduate School Monterey, California 93940	1
9.	Prof. Dale F. Leipper, Chairman, Code 58Lr Department of Oceanography Naval Postgraduate School Monterey, California 93940	1

10. Captain A. Skolnick 1
PMS 405
Naval Sea Systems Command
Washington, D. C. 20632

11. Lieutenant M. M. Hughes 3
PMS 405
Naval Sea Systems Command
Washington, D. C. 20632

12. Lieutenant W. L. Shutt 1
Oceanographic Unit Three
Fleet Post Office
San Francisco, California 96601

13. Lieutenant G. W. Karch 1
FWC Pearl Harbor
Fleet Post Office
San Francisco, California 96601

14. Department of Meteorology Library 1
Naval Postgraduate School
Monterey, California 93940